Hindawi
Mathematical Problems in Engineering
Volume 2020, Article ID 1486864, 16 pages
https://doi.org/10.1155/2020/1486864

Research Article

A Novel Modeling Method in Metal Strip Leveling Based on a Roll-Strip Unit

Guodong Yi, Zili Wang, and Zhouyu Hu

State Key Laboratory of Fluid Power & Mechatronic Systems, Zhejiang University, Hangzhou 310027, China

Correspondence should be addressed to Zili Wang; ziliwang@zju.edu.cn

Received 15 October 2019; Revised 29 October 2019; Accepted 18 December 2019; Published 31 January 2020

Academic Editor: Francesco Marotti de Sciarra

In the metal strip-multiroll leveling process, the action behavior of each roll is different. However, modeling each roll individually will result in redundancy which is not conducive to the modeling of the entire leveling process. To overcome this problem, a roll-strip unit (RSU) model is proposed to uniformly describe the behavior of each roll during the leveling process. The RSU and its equivalent model are defined on the basis of analyzing the force relationship between the roll and the strip. According to the linear distribution of the bending moment in the longitudinal direction of the strip, the position of the zero bending moment, that is, the virtual fulcrum, is obtained to determine the interval of the RSU. A plastic deformation function is established to describe the influence of plastic extension on the tension and velocity of the strip. The fitting of the deformation curve of the strip is optimized by the tension influence factor and the zero curvature moment. The static friction condition between the roll and the strip which ensures the normal operation of the RSU is given. The AMESim model of the RSU is established to lay the foundation for the dynamic modeling of the multiroll leveler.

1. Introduction

Precision metal strips are important materials with good mechanical properties and surface qualities in industrial production and are widely used in the manufacture of products in the aerospace, automotive, medical, electronics, and other industries.

Cold rolling and hot rolling are the main processing methods for metal strips and often cause flatness defects due to uneven internal stresses. As an effective tool to eliminate the flatness defects of metal strips, the multiroll leveler uses a set of rolls to bend the strips with different loads to achieve continuous leveling.

Currently, research on the leveling (straightening) methods for different types of metal profiles has focused on two aspects. One is the calculation of the leveling force parameters of the profile by the finite element method for designing the leveler. The other is the quality prediction and residual stress analysis of the leveled strips to obtain the optimum leveling parameters.

The rectilinear structure has the characteristics of a large length-diameter aspect ratio, so it has similar characteristics of the straightening process. In bar straightening, Wang et al. established a mathematical displacement-force model of the tension straightening process based on the elastic-plastic mechanics' theory and calculated the predicted displacement of tension straightening for various original deflections [1, 2]. Yu et al. established a quantitative analysis model and a finite element model of the two-roller straightening process and revealed the process mechanism of two-roller straightening [3]. Zhang et al. firstly proposed an asymmetrical hardening material model to describe the stress-strain curves considering the asymmetrical features of yield stress and plastic-hardening stage in tension and compression. The strain and stress distributions in elastic and plastic regions during the straightening process were discussed in their article [4]. Jin et al. researched the rotation blocking mechanism of the triple-roller equal curvature rotation blocking straightening system to solve the problem of bar rotation during the straightening process [5, 6]. In pipe straightening, Zhang et al. presented a simplified cantilever unit model and a mechanical model for calculating the straightening intermesh based on the structural features of the thin-walled tube and the numerical solution

of the finite element analysis (FEA) method [7, 8]. Zhang et al. studied the cross-sectional ovalization of the thin-walled circular steel tube during the straightening process, deduced simplified normal strain component formulas based on the thin shell theory, and presented a rational model for predicting the maximum section flattening of the thin-walled circular steel tube under its straightening process by the principle of minimum potential energy [9, 10]. In beam straightening, Yin et al. analyzed the multiroller straightening process of section steel based on the spring-back theory of small curvature plane bending and redefined the large deformation straightening strategy and the small deformation straightening strategy to improve the straightening quality [11]. Kaiser et al. established a beam with a rectangular cross section to consider the development of curvature during the straightening process and designed a trend of curvature intending to tailor the final residual stress distribution to the desired optimum [12]. Wang et al. proposed the load-deflection pressure straightening model to study the variation of the guide rail bending formation in the contiguous steps of the multistep straightening process through FEM and regression analysis [13].

In the plate leveling process, to obtain a flat product, the bending fibers or sections must be made straight from bending, and the residual stresses produced in the process of controlling material deformation must be eliminated [14, 15]. Liu et al. presented a new mechanics model based on the curvature integration method to predict the leveling process of plates and built an optimization model with equality and inequality constraints for the maximum yield stress search of each thickness of plates to judge whether incoming plates can be leveled quickly or not [16–18]. Cui et al. investigated the deformation characteristics and residual curvature during the longitudinal profile plate leveling process based on the curvature integral by elastic-plastic differences to solve the problem of changes in plate thickness [19]. Behrens et al. analyzed the edge and center waves of the sheet metal before and after deformation, investigated the effect of the leveling process on the sheet metal, and calculated the remaining shape defects after leveling [20]. Chen et al. investigated the essential deformation law of leveling for plates with transverse waves and proposed a 2.5-dimensional analytical model related to different initial unevenness to obtain the appropriate values of roller bending [21]. Brauneis et al. presented a fast and robust mathematical model for the leveling process of steel plates to calculate the leveling forces for a given plate and a given roll configuration of the leveler [22]. Among all the plate leveling processes, the heavy and composite plate leveling process is the most complex [23, 24]. Fan et al. established a stress neutral layer offset model based on three-point bending theory, steel plate bending characteristics, and layered theory in the straightening process to obtain the relationship between the neutral layer offset values and the reverse bending radius [25]. Baumgart et al. presented a detailed mathematical deflection model for heavy plate leveling to compensate for the effect of deflection on the roll intermesh and the plate flatness as well as to assess loads of critical parts [26].

The high yield strength of the metal strip material is high, which results in high tensile strength. It is hard for the straightening process. Zhang et al. researched the elastic-plastic deformation of a wide strip in tension leveling with the FEM, discovered the rules of tension leveling and the relations between elongation and technique factors, and obtained conclusions about tension leveling technology and tension leveler behaviors [27]. Maksimov et al. presented the tractive force exerted on strips with different mechanical properties by a straightening machine and determined how the tractive forces are affected by the cross-sectional area of the strip and the unit back tension [28]. Stadler et al. investigated the curvature and the contact force at the strip-roll contact point of a metal strip in an experimental device and derived a material model and a steady-state strip deformation model to compute the feasible combinations of curvature and contact force [29]. Grüber and Hirt proposed a control strategy on a force measurement in the first load triangle of a leveling machine and investigated a feedforward control strategy based on control curves for varying yield strengths along the strip length [30, 31]. Nikula et al. analyzed the mechanical stress inflicted on a roller leveler processing cold steel strips based on a feature extracted from vibration measurements and introduced models specific to different steel grades to the prediction of the stress level [32, 33].

The research mentioned above has made great progress in the leveling (or straightening) methods for different metal profiles. However, the action behavior of each roll on the strip is different in the multiroll leveling process, and modeling each roll individually will result in redundancy which is not conducive to the modeling of the entire leveling process. To describe the multiroll leveling process in a unified way, we propose an RSU model. To verify the effectiveness of the proposed model, we establish the RSU model in AMESim.

The remainder of this paper is organized as follows: The definition of the RSU based on the force analysis is firstly proposed in Section 2. Then, the virtual fulcrums of the RSU and the friction between the roll and the strip are analyzed in Section 3. In Section 4, the deformation curve is fitted and the deformation function of the strip is constructed. To verify the effectiveness of the proposed method, the RSU is modeled in AMESim and applied in the rolling production line in Section 5. At last, we draw conclusions in Section 6.

2. Definition of the RSU Based on Force Analysis

The multiroll leveling of strips can be abstracted as the interaction between the roll and the strip so that the roll and the strip section it acts on can be used as a basic component of the leveler, which is a roll-strip unit (RSU). To establish the RSU model, the force relationship between the roll and the strip during the leveling process is first analyzed, as shown in Figure 1.

In Figure 1, the strip applies a pressure P_i to the roll i and produces a torque R_i due to the friction between them. The strip is mainly affected by tension and bending moment,

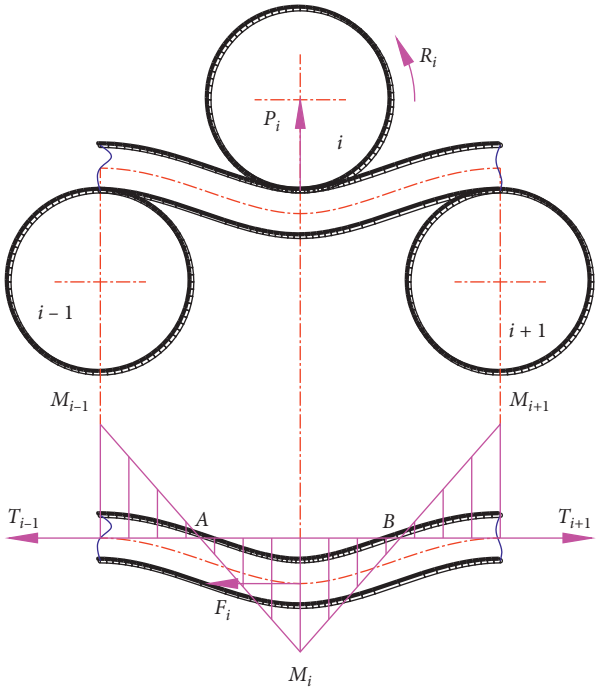

Figure 1: Force relationship between the roll and the strip.

without considering the effect of shear force. Within the length element, the force is shown in Figure 2.

Because the shear force is not considered, that is, $\sum Q = 0$, $dQ = 0$ and $Q' = (dQ/dx) = 0$. According to Figure 2, the bending moment of the strip element balanced, that is, $\sum M = 0$, so $Q = dM/dx$. Take the derivatives on both sides of the equation, then $M''(x) = 0$; that is to say, the bending moment is linearly distributed along the length in the strip. If M_{i-1}, M_i, and M_{i+1} are the maximum bending moments acting on the strips corresponding to the rolls i–1, i, and $i + 1$, respectively (the directions of M_{i-1} and M_{i-1} are opposite to that of M_i), the bending moments at the points A and B on the strip are zero, which are named virtual fulcrums. T_{i-1} and T_{i+1} are the forward and backward tensions of the strip segment, respectively. F_i is the static friction that the roll i acts on the strip.

Based on the above-mentioned analysis, an equivalent model of the RSU is established, as shown in Figure 3.

In the leveling process, the roll is regarded as a rigid body with a fixed rotation center due to its extremely small deformation, which can be equivalent to a set of moments of inertia and damping. The strip can be divided into elastic deformation sections and plastic deformation sections, and each of them is equivalent to a spring-damping system. Seven nodes are set between these sections, and velocities and tensions at these nodes are defined as v_1 to v_7 and T_1 to T_7, respectively. The length change of the strip caused by plastic deformation is represented by ξ, which is a function of the internal stress, the elastic modulus, and the speed difference between the two ends of the plastic deformation section. If there is no plastic deformation in the leveling, the length of the plastic deformation section l_P is 0. The drive unit of the roll is equivalent to a second-order system that

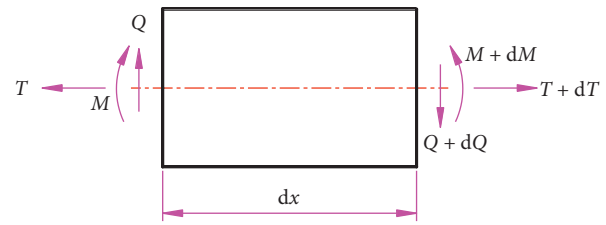

Figure 2: Force analysis of the strip element.

applies a speed or torque to the roll based on a control signal. α_i is the wrap angle of the strip on the roll. The key parameters and characteristics of the RSU model are discussed as follows.

3. Friction Analysis Based on RSU Virtual Fulcrums

3.1. Virtual Fulcrums of the RSU. According to the force analysis of the RSU, the bending moments are linearly distributed in the length direction of the strip with a maximum at the apex of the roll. The length direction of the strip is set to the X-axis, and x_i and x_{i+1} are the x-coordinates of the center point of the roll i and the roll $i + 1$, respectively, and $x_i = 0$ (i.e., the center of the roll $i + 1$ is at the coordinate origin). M_i and M_{i+1} are the maximum bending moments applied to the strip at the roll i and the roll $i + 1$, respectively. The x-coordinate of the virtual fulcrum B on the right side of the roll i is expressed as

$$B_X = \frac{x_{i+1}}{2} \cdot \frac{M_i}{M_i + M_{i+1}}. \tag{1}$$

The relationship between the bending moment and the deflection f_i of the strip is calculated by the Mohr integral method [34]:

$$f_i = \int_l K M_i dx, \tag{2}$$

where M_i is the bending moment generated by the unit force acting on the desired position.

According to the principle of material mechanics, in the elastic deformation range, the relationship between curvature and moment is

$$K = \frac{M}{EI}. \tag{3}$$

In the elastic-plastic deformation range, the relationship between curvature and moment is

$$K = \frac{M_W}{EI\sqrt{3 - 2(M/M_W)}}, \tag{4}$$

where M_W is the maximum elastic bending moment. When M is the maximum elastic bending moment, then equation (4) can be expressed the same as equation (3).

Equations (3) and (4) are substituted into equation (2) and integrated to obtain

$$f_i = f_W \Lambda^2 \left[5 - (3 + \Lambda)\sqrt{3 - 2\Lambda}\right], \tag{5}$$

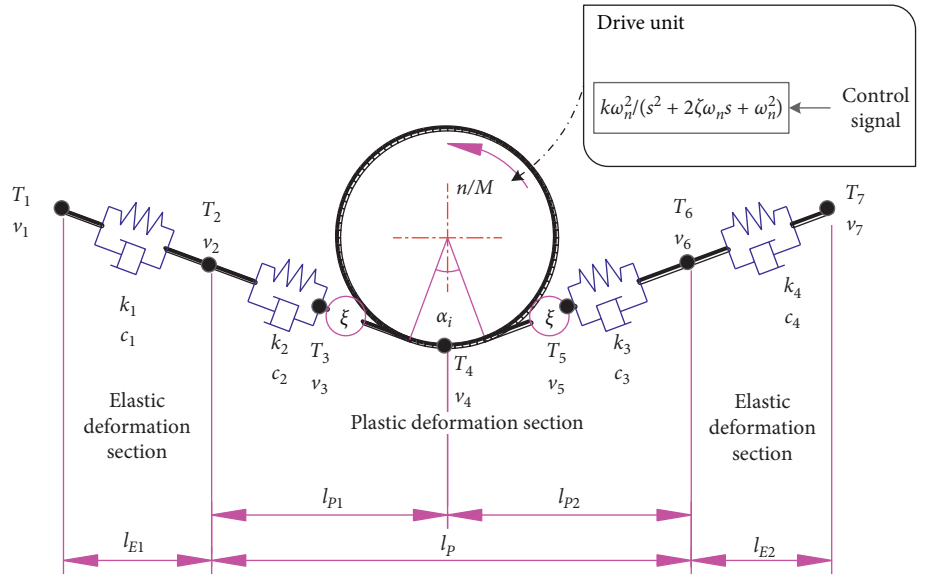

Figure 3: Equivalent model of the RSU.

where f_W is the maximum elastic bending deflection given as $f_W = A_X B_X M_W / 3EI$, in which A_X and B_X are the coordinates of the virtual fulcrums A and B, respectively, and $\Lambda = M_i / M_W f_W$.

Equation (5) determines the relationship between the total bending deflection f_i and the maximum bending moment M_i of the strip at the roll i. $f_i = f'_{i-1} + f''_i$, where f'_{i-1} is the residual deflection of the strip at the roll $i-1$ and f''_i is the reverse bending deflection of the strip at the roll i. f''_i is the sum of the residual curvature f'_i and the elastic recovery deflection $f_i^{''}$ of the strip at the roll i. The deformation deflection of the strip is shown in Figure 4.

During the leveling process, the original curvature of the strip and the relative position between rolls are known, so the total bending deflection f_i of the strip at each roll can be calculated. If the final curvature of the strip after leveling is zero, i.e., the strip is completely leveled, the positions of virtual fulcrums can be calculated by the iteration method, as shown in Figure 5.

3.2. Friction between the Roll and the Strip. In the RSU, the speed of the roll and the strip must be the same at the contact point; otherwise, there will be relative sliding between them, which will affect the surface quality of the strip and the service life of the roll. Therefore, the friction between the roll and the strip is static and depends on the speed relationship between them.

A microelement of the strip at the point of contact with the roll is taken out for force analysis, as shown in Figure 6.

When the difference between the tensions acting on the strip section corresponding to the wrap angle on the roll is $\Delta T = T_5 - T_3$, the difference between the tensions acting on the microelement corresponding to the angle $d\alpha$ is

$$T' - T = \frac{\Delta T}{r(\alpha_1 + \alpha_2)} \cdot r\, d\alpha = \frac{d\alpha}{\alpha_1 + \alpha_2} \Delta T. \quad (6)$$

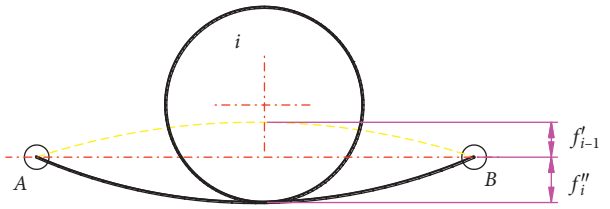

Figure 4: Deformation deflection of the strip.

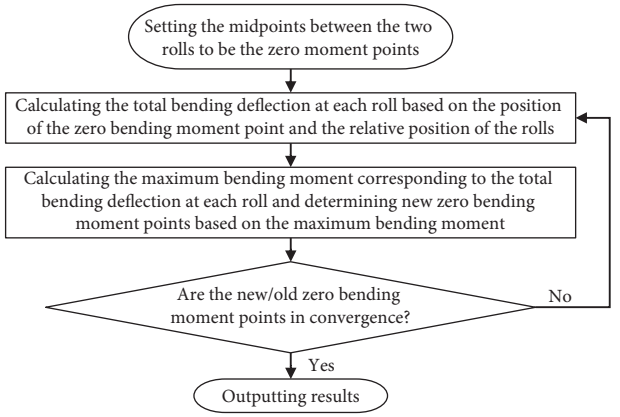

Figure 5: Solution process of the zero bending moment point of the strip.

Since the strip deformation is continuous, the distribution of the leveling force on the strip is fairly smooth, so for the convenience of calculation, the leveling force applied by the roll to the strip can be considered a linear distribution, as shown in Figure 7.

If the strip width is a unit size, the area of the triangle in Figure 7 is equal to the total leveling force P, and the maximum leveling force P_m is

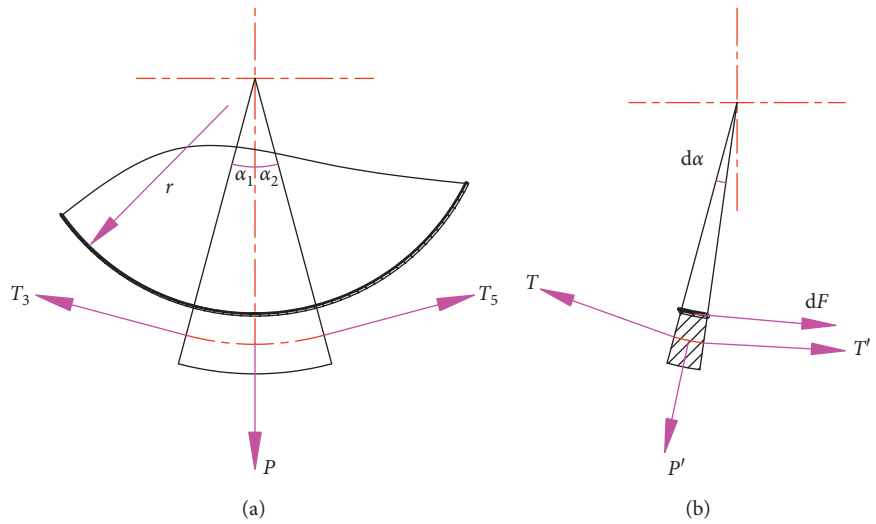

Figure 6: Forces acting on the microelement of the strip.

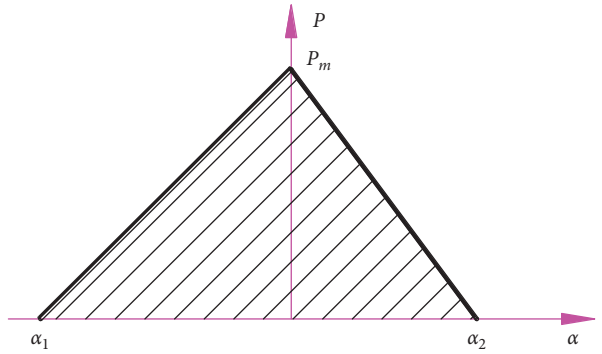

Figure 7: Distribution of leveling force.

$$P_m = \frac{2P}{\alpha_1 + \alpha_2}. \tag{7}$$

Once P_m is determined, the distribution curve of leveling force is also determined. The force relationship of the microelement is expressed as

$$dF + T' - T + ma = dF + \frac{d\alpha}{\alpha_1 + \alpha_2} \cdot T + \rho_l r\, d\alpha \cdot a = 0. \tag{8}$$

Equation (8) is derived as follows:

$$dF = -\left(\frac{\Delta T}{\alpha_1 + \alpha_2} + \rho_l r a\right) d\alpha. \tag{9}$$

Equation (9) is integrated to obtain the static friction F:

$$F = -\int_0^{\alpha} \left(\frac{\Delta T}{\alpha_1 + \alpha_2} + \rho_l r a\right) d\alpha = -\Delta T - \rho_l r (\alpha_1 + \alpha_2) a. \tag{10}$$

The maximum static friction between the strip and the roll is

$$F_{\max} = -\int_0^{\alpha} P'(\alpha) \mu\, d\alpha, \tag{11}$$

where $P'(\alpha)$ is used to represent the positive pressure P' acting on the microelement. The normal working condition of the RSU is $F < F_{\max}$.

4. Analysis of the Strip Deformation

4.1. Fitting of the Deformation Curve. The length of the strip section in the RSU and its wrap angle on the roll are determined by the deformation curve of the strip in leveling.

Traditional curve fitting methods consider that the strip and the roll are in line contact, and the influence of the tension is not taken into account in the calculation. However, the deformation curve is greatly affected by the tension in practice, and the wrap angle is not zero. In this paper, an improved curve fitting method based on traditional methods is proposed to make the fitting curve closer to the actual deformation curve, as shown in Figure 8.

Suppose the strip tension is small enough, the contact between the roll and the strip is a point. In this case, the strip deformation is continuous and the deformation curve is continuous and smooth everywhere with the first- and second-order continuity at the discontinuity point. A quartic polynomial $y = ax^4 + bx^3 + cx^2 + dx + e$ with to-be-

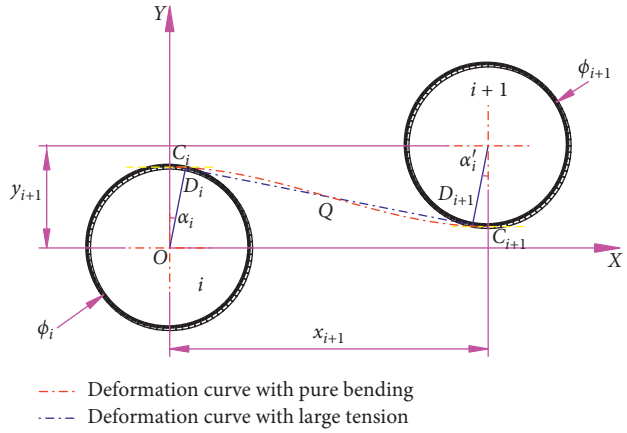

Figure 8: Improved fitting of the deformation curve.

determined coefficients is used to fit the deformation curve of the strip with pure bending [35], as shown by the red line in Figure 8. The first-order derivatives at points C_i and C_{i+1} and the second-order derivatives at point B are all zero. The following equation is derived based on the illustrated geometric relationships:

$$\begin{cases} y = ax^4 + bx^3 + cx^2 + dx + e\big|_{x=0} = \dfrac{\phi_i}{2}, \\ y = ax^4 + bx^3 + cx^2 + dx + e\big|_{x=x_{i+1}} = y_{i+1} - \dfrac{\phi_{i+1}}{2}, \\ y' = 4ax^3 + 3bx^2 + 2cx + d\big|_{x=0} = 0, \\ y' = 4ax^3 + 3bx^2 + 2cx + d\big|_{x=x_{i+1}} = 0, \\ y'' = 12ax^2 + 6bx + 2c\big|_{x=B_X} = 0. \end{cases} \tag{12}$$

Equation (12) is solved as follows:

$$\begin{cases} a = \dfrac{3(x_{i+1} - 2B_X)(\phi_i + \phi_{i+1} - 2y_{i+1})}{2x_{i+1}^3(6B_X^2 - 6B_X x_{i+1} + x_{i+1}^2)}, \\ b = \dfrac{2(3B_x^2 - x_{i+1}^2)(\phi_i + \phi_{i+1} - 2y_{i+1})}{x_{i+1}^3(6B_X^2 - 6B_X x_{i+1} + x_{i+1}^2)}, \\ c = \dfrac{3B_X(2x_{i+1} - 3B_X)(\phi_i + \phi_{i+1} - 2y_{i+1})}{x_{i+1}^2(6B_X^2 - 6B_X x_{i+1} + x_{i+1}^2)}, \\ d = 0, \\ e = \dfrac{\phi_i}{2}. \end{cases} \tag{13}$$

When there is tension in the leveling and the tension is large enough, the deformation curve of the strip is changed, as shown by the blue line in Figure 8, which is fitted by the arc-tangent-arc, and the tangent points are D_i and D_{i+1}, respectively. The theoretical half wrap angles of the strip on the rolls are α_i and α_i', respectively. Therefore, the deformation curve of the strip is completely determined by the coordinates of the two tangent points. The coordinates of D_i and D_{i+1} are (x_0, y_0) and (x_1, y_1), respectively, and the following equation is obtained according to the geometric relationship mentioned above:

$$\begin{cases} x_0^2 + y_0^2 = \dfrac{\phi_i^2}{4}, \\ (x_1 - x_{i+1})^2 + (y_1 - y_{i+1})^2 = \dfrac{\phi_{i+1}^2}{4}, \\ \dfrac{y_0}{x_0} \cdot \dfrac{y_1 - y_0}{x_1 - x_0} = -1, \\ \dfrac{y_1 - y_0}{x_1 - x_0} \cdot \dfrac{y_1 - y_{i+1}}{x_1 - x_{i+1}} = -1. \end{cases} \tag{14}$$

Theoretical half wrap angles are calculated according to equation (14) as follows:

$$\alpha_i = \alpha_i' = \arctan\left(\frac{x_0}{y_0}\right). \tag{15}$$

Strip deformation with pure bending and that with large tension are two extreme cases of actual deformation. Therefore, the actual deformation curve of the strip is located in the space surrounded by the two curves formed by the two extreme cases and cross intersection point Q of these two curves.

If the distance between two rolls is small and the intermesh of the roll is large, a part of the strip will also completely fit the roll to form a wrap angle even if the strip is purely bent. Therefore, on the basis of the traditional curve fitting method, this paper introduces a tension factor λ to optimize the fitting curve. The improved algorithm flow is shown in Figure 9.

The tension factor λ is mainly affected by the strip stiffness, the tension, and the roll diameter and can be obtained by experiment and interpolation with the value range $[0, 1)$. λ increases with the increase of tension, decreases with the increase of stiffness, and increases with the increase of roll diameter. In leveling practice, the strip stiffness and the roll diameter are constant, so the tension plays a major role.

The strip is assumed to be tangent to the rolls at both the entrance and the exit of the leveler; then, the deformation curve of the strip is obtained and denoted as $y(x)$ via the curve fitting algorithm proposed above. The curvature of any point on the strip deformation curve $y = y(x)$ can be calculated as

$$\frac{1}{\rho} = \frac{|y''|}{(1 + y^2)^{(3/2)}}. \tag{16}$$

By fitting the deformation curve of the strip, the deformation curvature at any point of the strip and the wrap angle on each roll are obtained, which are the necessary parameters for dynamic modeling of the RSU.

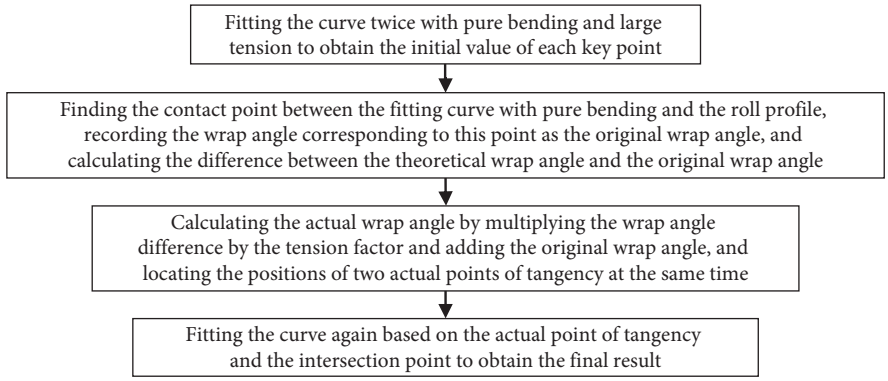

Figure 9: Improved curve fitting algorithm.

4.2. Deformation Function of the Strip. When the deformation stress is less than the yield stress, the strip is elastically deformed; otherwise, the strip is plastically deformed. Elastic deformation is recoverable, while plastic deformation is unrecoverable and has an effect on the movement speed of the strip. The deformation of the strip in the RSU may be only elastic or both elastic and plastic depending on the stress distribution. Therefore, as long as the length of the plastic deformation section of the strip is determined, the length of the elastic deformation section is also determined.

A microelement is taken from the strip for analysis. The main stress acting on the microelement is tension T and bending moment M. The stress distribution of the microelement obtained by superimposing these two stresses is shown in Figure 10, where ε_p denotes the tension elongation rate and ε_s denotes the bending elongation rate [34].

In Figure 10, when the tension and the bending moment act on the microelement, the deformation neutral layer deviates from the thick symmetric layer with a distance a_h. According to the force balance condition in the horizontal direction, it can be concluded as equation (17.1) and can be further simplified as equation (17.2):

$$\frac{a_h + (h/2)}{a_h - (h/2)} = \frac{\varepsilon_s + \varepsilon_p}{\varepsilon_s - \varepsilon_p}, \tag{17.1}$$

$$a_h = \frac{h}{2} \cdot \frac{\varepsilon_s}{\varepsilon_p}. \tag{17.2}$$

According to the fitting curve of the deformed strip, the bending stress distribution inside the strip can be obtained by the flow shown in Figure 9. Since the initial curvature of the strip is substantially uniform in mass production, the total bending deflection of the strip at the roll can be considered constant during leveling; that is, the bending moment inside the strip is constant.

The tension is calculated by the velocity difference between adjacent velocity nodes. The change of the tension acting on the strip between velocity nodes v_i and v_{i+1} from time t_0 to t_1 is expressed as

$$\Delta T = T_{i+1} - T_i = \frac{sE}{l} \int_{t_0}^{t_1} (v_{i+1} - v_i) \mathrm{d}t, \tag{18}$$

where $l = \int_{x_i}^{x_{i+1}} \sqrt{1 + y'^2} \mathrm{d}x$. Since the initial value of the tension acting on the strip is 0, the tension acting on each segment at any time is determined by the velocity-time function $v_i(t)$ of each node.

Based on the known bending moment and tension, the stress at any position of the strip at any time can be determined by superimposing the bending stress and the tensile stress, and the elastic and plastic deformation sections can be determined depending on whether the stress exceeds the material yield limit. The plastic deformation of the strip consumes energy and may cause an extension in the length direction. The work done by external force in leveling is equal to the work done by internal force. If a strip with a length ds is bent from the curvature $1/R_1$ to $1/R_2$, the work $\mathrm{d}A$ done by the bending moment M acting on the strip is [34]

$$\mathrm{d}A = M\left(\frac{\mathrm{d}s}{R_2} - \frac{\mathrm{d}s}{R_1}\right) = M\,\mathrm{d}s\left(\frac{1}{R_2} - \frac{1}{R_1}\right). \tag{19}$$

For a strip with the abscissa from x_i to x_{i+1}, when the total bending curvature is $1/R$ and the springback curvature is $1/\rho$, the work done by the bending moment M is

$$A = Ml\left(\frac{1}{R} - \frac{1}{2\rho}\right) = M \int_{x_i}^{x_{i+1}} \sqrt{1 + y'^2} \mathrm{d}x \cdot \left(\frac{1}{R} - \frac{1}{2\rho}\right). \tag{20}$$

Because part of the energy in A is returned to the system due to the springback of the strip, the actual consumed power A_p is

$$A_p = M \int_{x_i}^{x_{i+1}} \sqrt{1 + y'^2} \mathrm{d}x \cdot \left(\frac{1}{R} - \frac{1}{\rho}\right). \tag{21}$$

In the range of the abscissa (x_i, x_{i+1}), the work A_ξ required for the length extension of the strip is

$$A_\xi = \sigma_s bhl\xi = \sigma_s bh \int_{x_i}^{x_{i+1}} \sqrt{1 + y'^2}\, \xi(x) \mathrm{d}x. \tag{22}$$

Because the tension and the bending moment act together on the strip, the deformation neutral layer deviates from the thick symmetric layer with a distance a, and the thick symmetric layer is stretched. If the stretch is plastic, the strip is extended. The tensile deformation of the thick

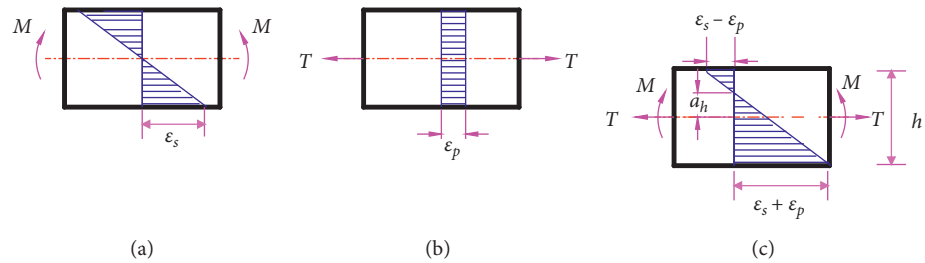

Figure 10: Stress distribution of a strip microelement. (a) Stress distribution with bending moment. (b) Stress distribution with tension. (c) Stress distribution with bending moment and tension.

symmetric layer plays an important role in improving the strip shape, but it is difficult to quantitatively calculate the deformation. At present, it is considered that the strip is plastically extended only when the thickness of the one-sided elastic deformation z_0 is less than a, and the plastic deformation ε_r of the thick symmetric layer of the strip is as follows [34]:

$$\varepsilon_r = \frac{\sigma_s}{E}\left(\frac{\sigma_p}{\sigma_s}K_z - 1\right)\left[1 - \frac{\eta(K_z - 1)}{\left(1 + \left(\sigma_p/\sigma_s\right)\right)K_z - 1}\right]. \quad (23)$$

The elongation rate $\xi(x)$ at a point $(x, y(x))$ on the fitting curve is

$$\xi(x) = \frac{\sigma_s}{E}\left(\frac{a(x)}{z_0(x)} - 1\right)\left[1 - \frac{\eta\left(\left(h/2z_0(x)\right) - 1\right)}{\left(1 + (2a(x)/h)\right)\left(h/2z_0(x)\right) - 1}\right]. \quad (24)$$

5. AMESim Modeling of the RSU and Its Application in Rolling Production Line

5.1. AMESim Modeling of the RSU. According to the RSU model defined above, AMESim is used to implement the dynamic modeling, as shown in Figure 11. The "roll/strip contact calculation unit" is a custom-developed component, which will be described below. The strip is divided into four mass-spring-damping segments, corresponding to four deformation sections. The motor is driven by a control signal, acts on a roll system with an equivalent rotational inertia of J via a spring-damping system, and finally acts on the strip by a roll. Adjacent RSUs are coupled by speed.

The force relationship between the roll and the strip includes two aspects: one is the bending moment and the force at the contact point of the strip and roll in the tangential direction applied to the strip by the roll and the other is the additional torque applied to the roll by the strip. According to the analysis of the force relationship between the roll and the strip, the implementation of the "roll/strip contact calculation unit" is shown in Figure 12.

AMECustom is used to customize and package the RSU to establish a new basic element and its submodel, as shown in Figure 13, which is also one of the basic components for building the AMESim model of a leveler.

5.2. RSU Application in Rolling Production Line AMESim Modeling. The rolling production line is a highly integrated set of equipment which is designed and customized according to the process requirements of customers and the layout of the specific production environment [36]. Different rolling production lines contain different equipment and different layout of equipment; nevertheless, the rolling production line must contain the following basic equipment: uncoiler, pinch roller, rolling machine, tension roller, and winder. The basic equipment in the rolling production line is shown in Figure 14.

5.2.1. Uncoiler and Winder. Due to the working stability, the uncoiler and the winder can be, respectively, defined as a single-input and a single-output roll/strip basic unit, as shown in Figure 15. This process is also considered to simplify the modeling and improve the simulation speed.

5.2.2. Pinch Roller. The pinch roller can be simplified as a basic roll/strip unit. According to the working principle of the pinch roller, the positive pressure is applied by the lower roller to the upper roller, which is irrelevant to the bending deformation of the strip, and is constant in the working process. When the strip passes through the pinch roller, the wrap angle is very small, approximating to zero. Considering the working state of the whole production line, there is no plastic deformation area in the equivalent roll/belt basic unit where the pinch roll is located. The AMESim model and its customized components of the pinch roller are shown in Figure 16.

5.2.3. Tension Roller. The principle of the tension roller is that when the strip is wrapped around the tension roll, the friction force is produced in the contact arc, which enlarges or reduces the tension of the strip at the entrance and exit of the tension roll. In the production process, the practical wrap angle is always smaller than its theoretical value, and with the increase of plate stiffness, the practical wrap angle is smaller. The AMESim model and its customized components of the tension roller are shown in Figure 17.

5.2.4. Multiroller Leveling Machine. At present, most of the multiroller leveling machines are second-generation or second-and-a-half-generation products. In the mechanical

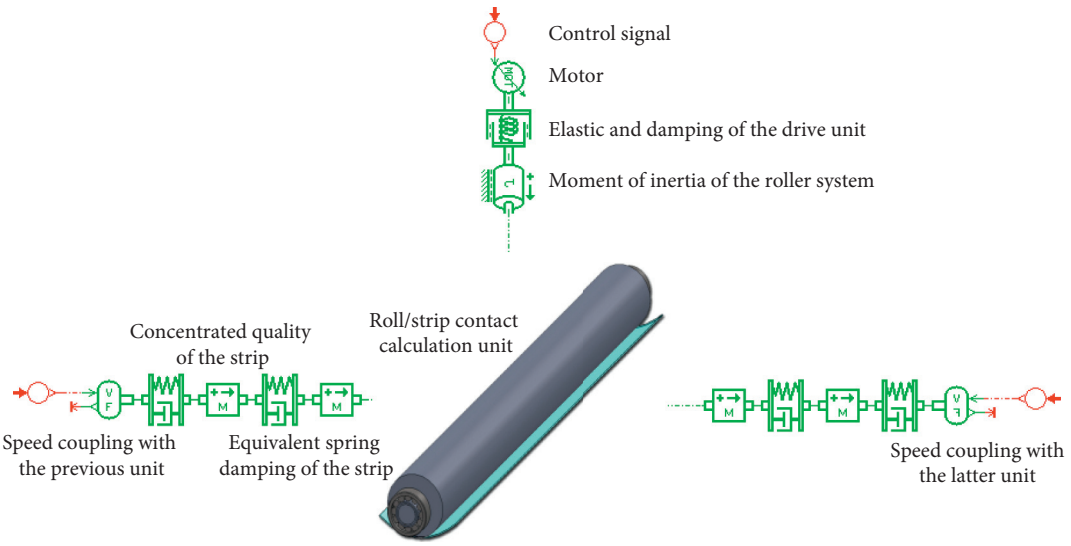

Figure 11: Dynamic model of the RSU implemented in AMESim.

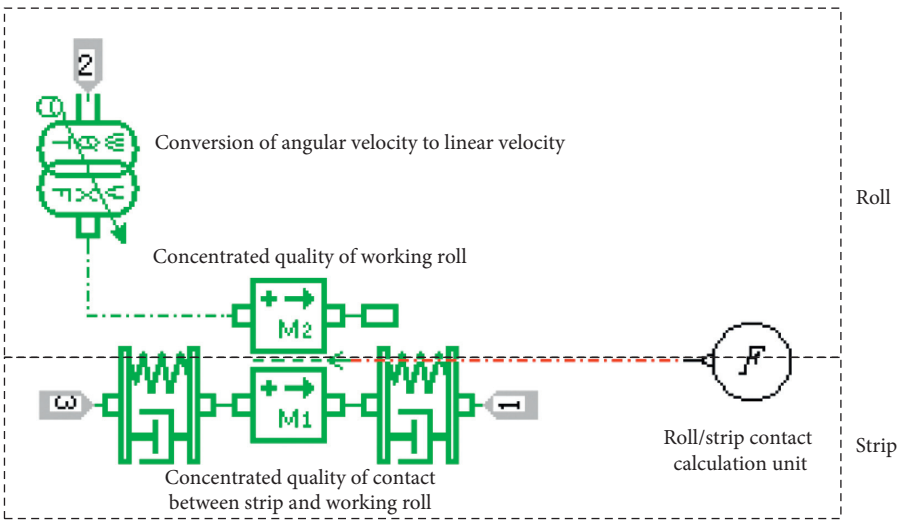

Figure 12: Roll/strip contact calculation unit.

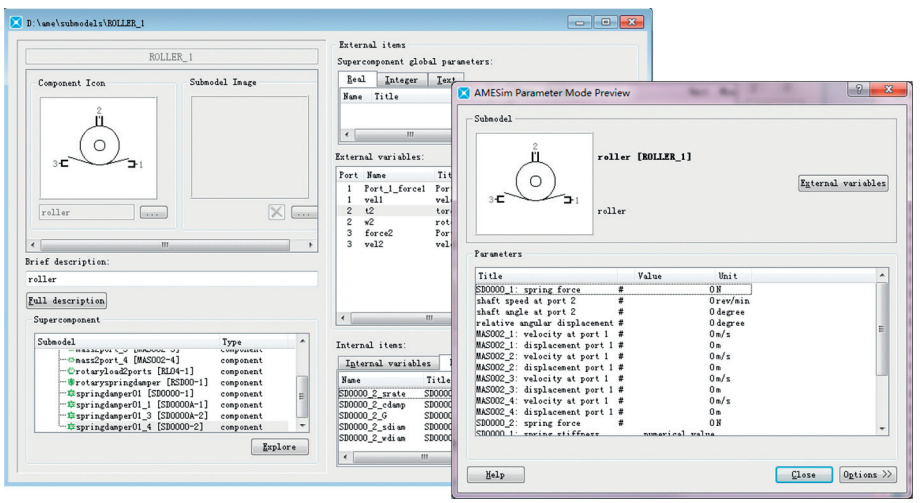

Figure 13: Customization of the RSU.

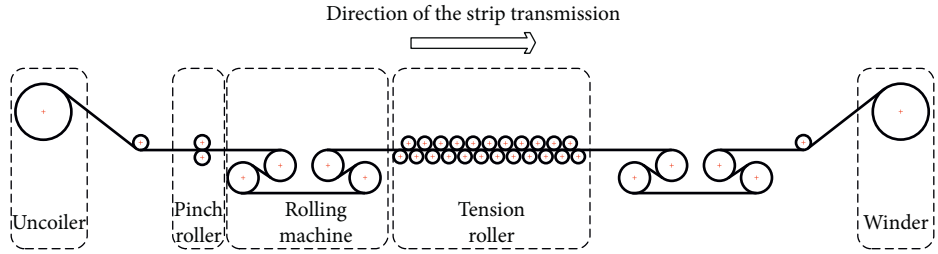

Figure 14: Typical equipment in the rolling production line.

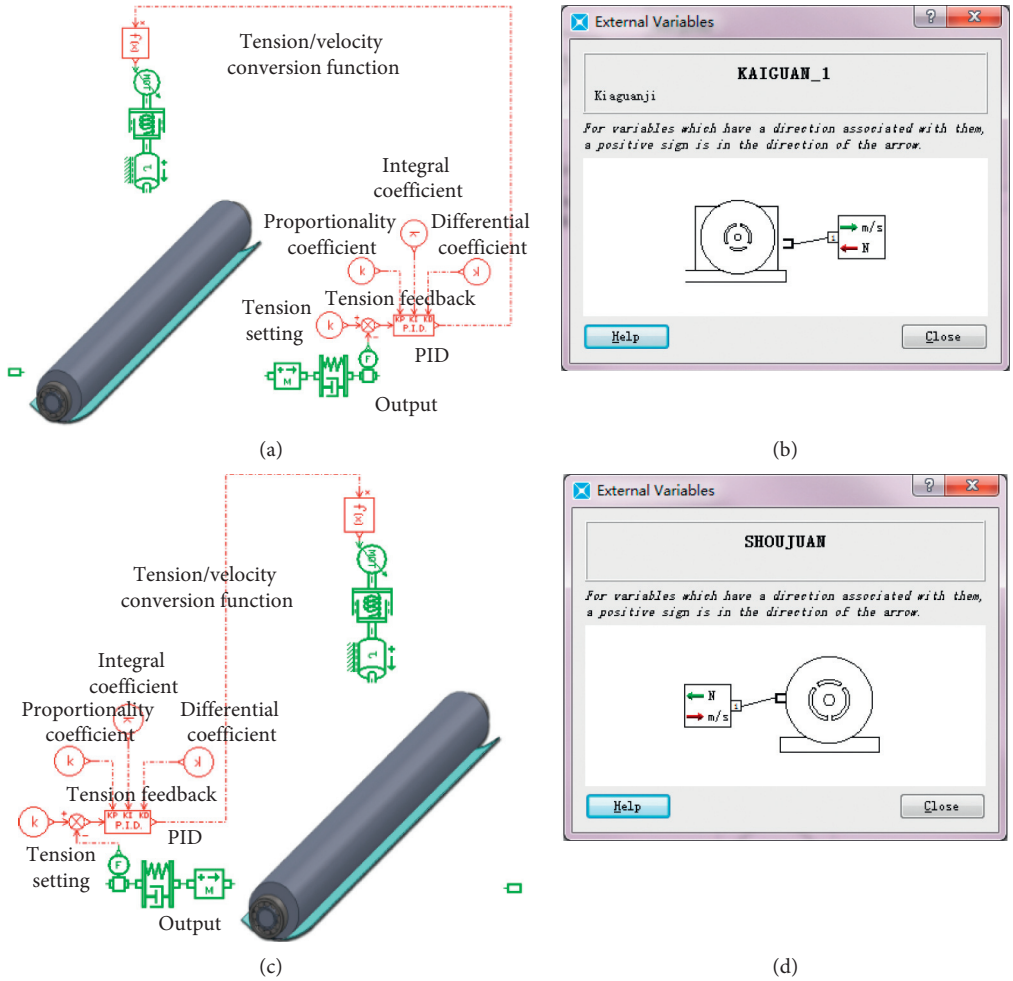

Figure 15: Uncoiler: (a) AMESim model and (b) customized components; winder: (c) AMESim model and (d) customized components.

configuration, the diameter of the working roll is uniform. The centralized driving mode is adopted in the traditional systems. The working rollers are driven by a high-power motor through coupling, gearbox, and universal coupling. The reduction of the roll system is adjusted by the inclination and reduction of the upper roll system. We take a 23-roller leveling machine designed and manufactured by Boya Precision Industrial Equipments Co., Ltd., as an example to illustrate the multiroller leveling machine modeling process using the RSU. The AMESim model and its customized components of the multiroller leveling machine are shown in Figure 18.

To synthesize the above modeling, we can obtain the whole rolling production line AMESim modeling, as shown in Figure 19.

5.3. Rolling Production Line Association Modeling System. The rolling production line AMESim modeling based on the RSU is utilized in developing the rolling production line association modeling system. The modeling system integrates MATLAB into the dynamic model of the rolling production line in AMESim. It helps to assign parameters, to read variables, and in simulation control. The specific

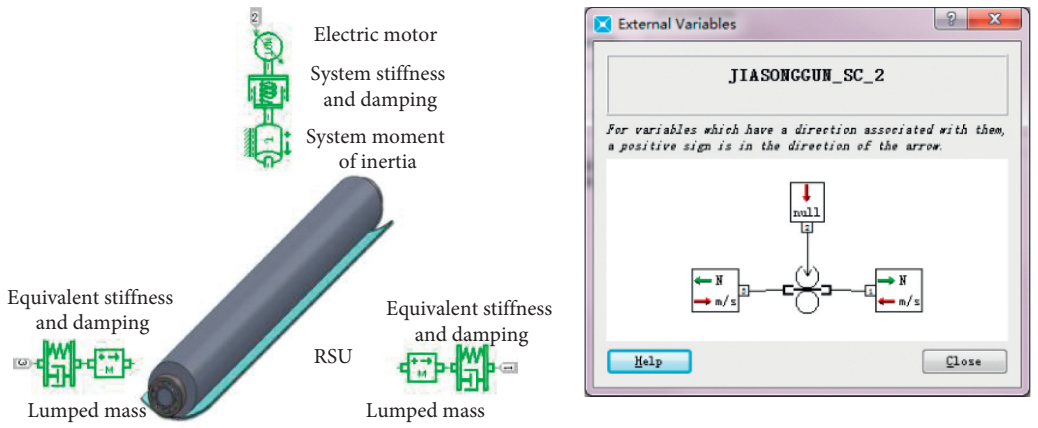

(a) (b)

Figure 16: Pinch roller: (a) AMESim model and (b) customized components.

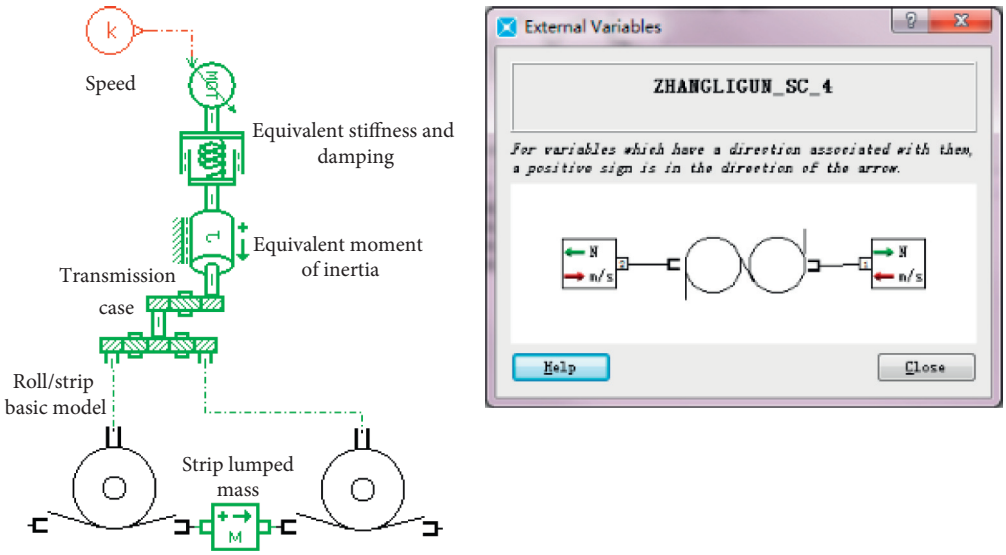

(a) (b)

Figure 17: Tension roller: (a) AMESim model and (b) customized components.

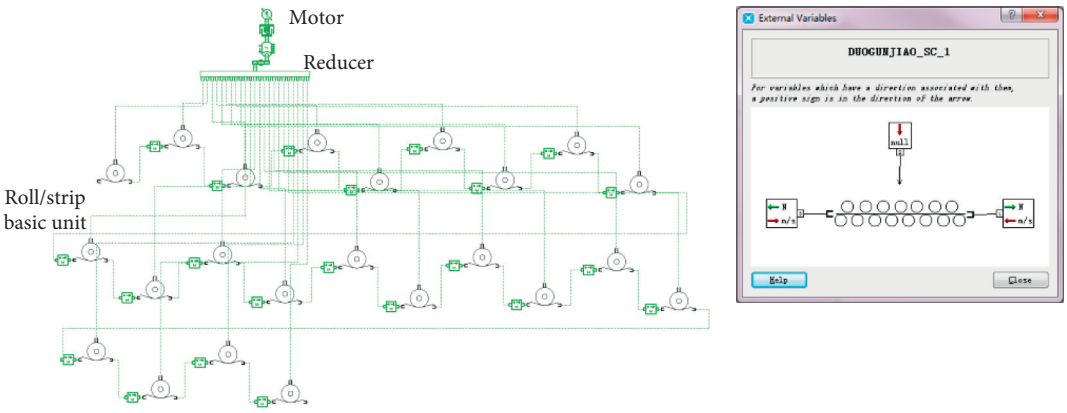

(a) (b)

Figure 18: Multiroller leveling machine: (a) AMESim model and (b) customized components.

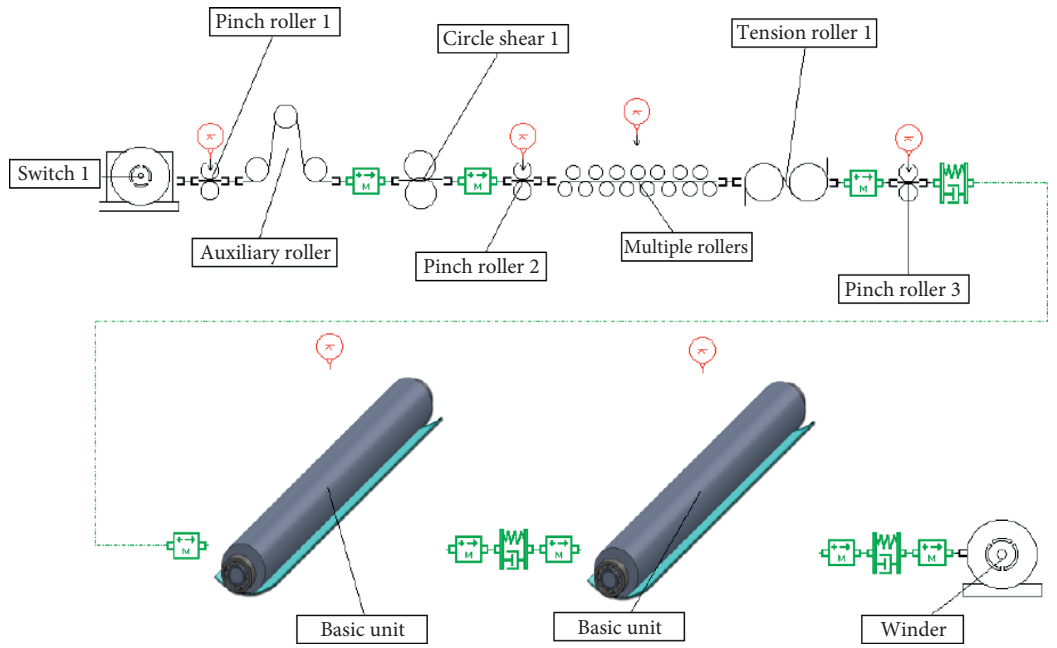

Figure 19: Whole rolling production line AMESim modeling.

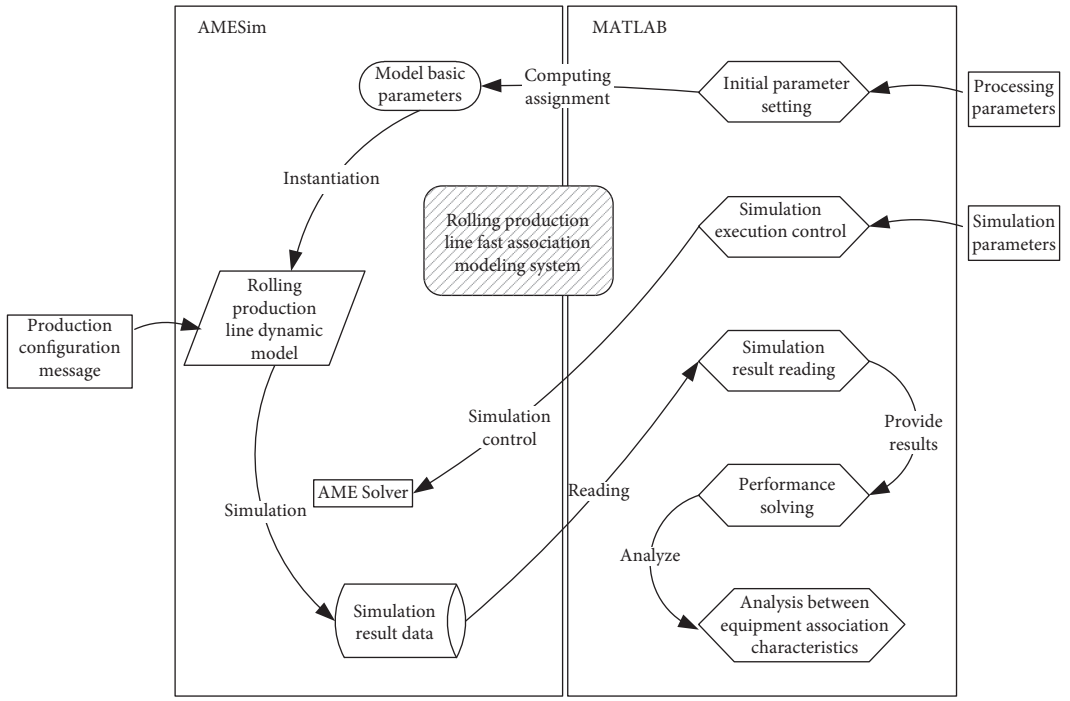

Figure 20: Framework of the rolling production line fast association modeling system.

framework of the rolling production line fast association modeling system is shown in Figure 20.

The initial parameter setting module calculates the parameters of each basic functional unit in the model according to the input information, including the inherent parameters of the equipment (roll diameter, roll distance, etc.) and the processing parameters (downpressure, strip material, and design tension). It is also responsible for transmitting the specific values of the corresponding parameters to the AMESim model after the calculation is completed. The parameters and variables of each submodel in the AMESim model can be found through a unique handle and read and write. When this module is initially executed, it will require basic information of the straightening production line model, including the model file name and device corresponding to the model instance name. Then, it can automatically update model parameters when it is executed again. The wizard parameter setting method is

Figure 21: Basic information of the rolling production line.

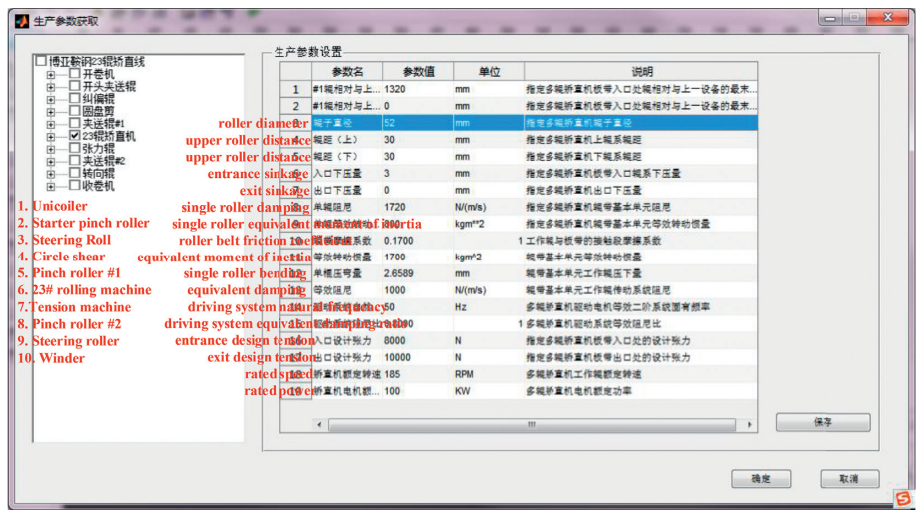

Figure 22: Process parameters of the rolling production line.

provided in the module to ensure the accuracy of the parameter input. The basic information of the rolling production line can be obtained in the function module shown in Figure 21. The process parameters of the rolling production line can be obtained in the function module shown in Figure 22. After obtaining the basic parameters, the simulation process can be implemented. In the process of simulation, the parameters of the model are not a constant but a function of other parameters because of the elastic-plastic deformation of the strip. It may change in the process of simulation; for example, the length of the elastic interval of the strip may change when the tension changes. The function of the simulation execution control module is to recalculate the parameters and set the model after each step of simulation within a given integration time interval so as to achieve the purpose of making the simulation results more accurate. It should be pointed out that the efficiency of reading AMESim results in the MATLAB environment is low, so the module also provides the reading frequency control options for the simulation results. Figure 23 shows the setting function of the simulation execution module.

AMESim returns the simulation results to MATLAB in the form of two matrices at the end of each simulation stage, one of which is the result matrix, which saves the final values of all variables in the model at the end of simulation, and the other matrix saves the name information of all variables. When the information is transmitted to the platform, it needs to be decoded by the recognition module read by the simulation results to identify the required information and provide it to other modules for use, as shown in Figure 24. Take tensor calculation at each node as an example. According to equation (12), the tensor difference between node 1 and node 2 can be calculated as

$$\Delta T = T_2 - T_1 = \frac{sE}{l}\int_{t_1}^{t_2}(v_2 - v_1)\mathrm{d}t = 20.1\,\mathrm{N}, \tag{25}$$

where s and E are obtained in the module shown in Figure 21. The strip length between nodes can be calculated

Figure 23: Simulation execution module.

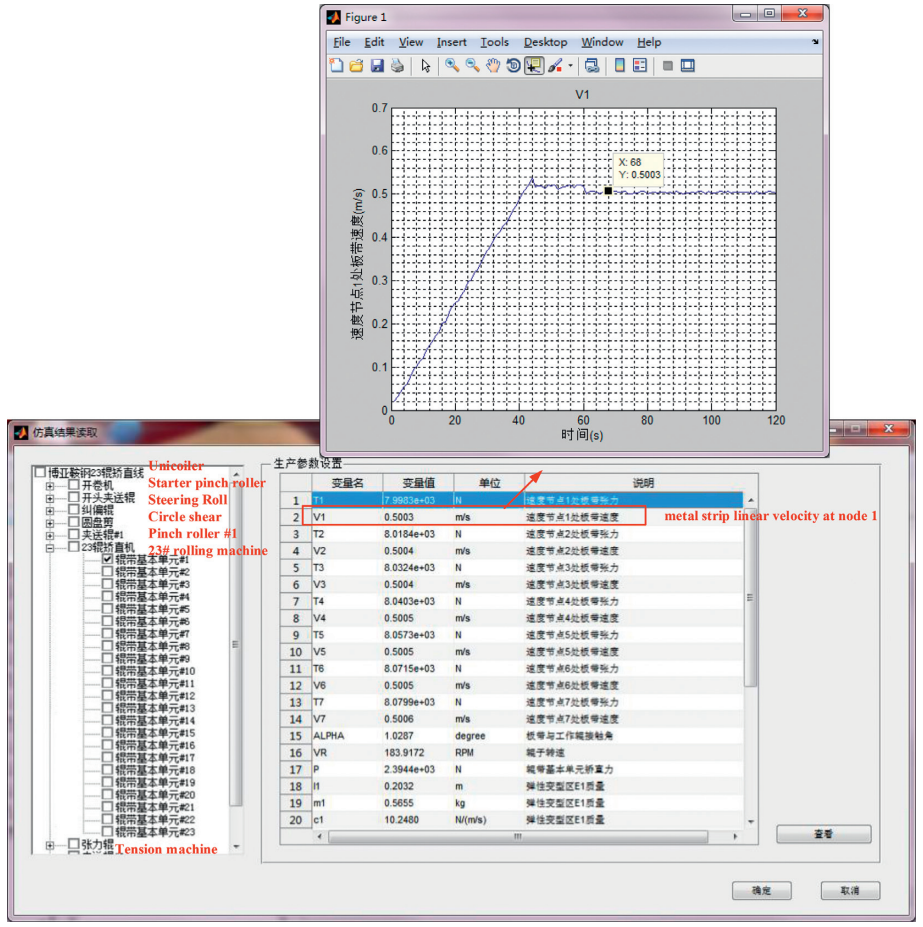

Figure 24: Simulation result reading module.

as $l = \int_{x_1}^{x_2} \sqrt{1 + y'^2}\,dx$, where y' is expressed based on equations (6) and (7). So on the premise that T_1 is known, we can obtain T_2. Analogically, the tensions at other nodes are calculated and shown in the module in Figure 24. With the help of the rolling production line association modeling system based on the RSU, the parameter information of the complex multiroll leveling manufacturing system can be obtained more conveniently and the related performance parameters can be calculated quickly, which is helpful to realize the digitalization of the complex multiroll leveling manufacturing.

AMESim is a graphic modeling and simulation software program based on power flow data. For the convenience of calling, AMECustom is used to customize the RSU AMESim

modeling process. It not only facilitated the centralized setting of submodel parameters but also reduced the complexity of subsequent processes. By analyzing the working principle of each equipment in the rolling production line, the dynamic model can be built in AMESim. Finally, the dynamic model database of the rolling equipment is established, and it helps to create the dynamic model of the rolling production line more efficiently.

6. Conclusions

In this paper, a roll-strip unit is proposed for the unified modeling of multiroll leveling for metal strips. The virtual fulcrums of the unit are defined based on the force analysis of the RSU. To analyze the friction between the roll and the strip, the deformation curve of the strip is fitted and the deformation function is constructed. The strip deformation with pure bending and that with large tension are two extreme cases of actual deformation, and the actual deformation curve of the strip is located in the space surrounded by the two curves formed in the two extreme cases. The elastic deformation of the strip is recoverable, while plastic deformation is unrecoverable and has an effect on the movement speed of the strip.

The plastic deformation of the strip consumes energy and may cause an extension in the length direction, which plays an important role in improving the strip shape. The friction between the roll and the strip is static, and it depends on the speed relationship between them. The RSU is modeled in AMESim. It is applied in a 23-roller rolling production modeling. With the help of the rolling production line association modeling system based on the RSU, the parameter information of the complex multiroll leveling manufacturing system can be obtained more conveniently and the related performance parameters can be calculated quickly, which is helpful to realize the digitalization of the complex multiroll leveling manufacturing [36].

Nomenclature

a: Acceleration of the microelement
$a(x)$: Deviation of the thick symmetric layer
b: Width of the strip
E: Elastic modulus of the material
F: Static friction
h: Thickness of the strip
I: Section inertia moment of the material
K: Bending curvature of the strip
K_z: Relative bending curvature
l: Length of the strip between the nodes
M: Bending moment
P: Total leveling force
P_m: Maximum leveling force
Q: Shear force
R: Bending radius
s: Sectional area of the strip
T: Tension force
$v_i(t)$: Velocity-time function
$z_0(x)$: One-sided elastic deformation on the x-axis
η: Material-strengthening coefficient
Λ: Bending moment coefficient
λ: Tension factor
ρ: Radius of the curvature
σ_p: Material tensile stress
σ_s: Material yield stress
$\xi(x)$: Elongation function of the strip
ε_r: Plastic deformation
ρ_l: Linear density of the strip
μ: Maximum static friction factor between the strip and the roll.

Data Availability

The data used to support the findings of this study are included within the article.

Conflicts of Interest

The authors declare that they have no conflicts of interest.

Acknowledgments

This work was supported by the National Key R&D Program of China (grant no. 2018YFB1701601) and the National Natural Science Foundation of China (grant no. 51875515).

References

[1] X. Wang, D. Zhang, J. Peng et al., "Mathematical model of tension straightening process and its experiment validation," *Journal of Mechanical Engineering*, vol. 47, no. 8, pp. 66–370, 2011.

[2] J. Yan, D.-F. Zhang, X.-H. Wang et al., "The mathematic model of tension straightening process of magnesium alloy and experimental validation," *Journal of Magnesium and Alloys*, vol. 1, no. 1, pp. 76–81, 2013.

[3] G. Yu, R. Zhai, J. Zhao, and R. Ma, "Theoretical analysis and numerical simulation on the process mechanism of two-roller straightening," *The International Journal of Advanced Manufacturing Technology*, vol. 94, no. 9–12, pp. 4011–4021, 2018.

[4] Y. Q. Zhang, H. Lu, X. B. Zhang et al., "A novel analytical model for straightening process of rectangle-section metal bars considering asymmetrical hardening features," *Advances in Mechanical Engineering*, vol. 10, no. 9, Article ID 168781401879915, 2018.

[5] H. Jin and X. Lu, "Inflection moment calculation and resilience analysis of roller straightening," *Functional Materials*, vol. 23, pp. 138–145, 2016.

[6] Y. L. Yi and H. R. Jin, "Three roller curvature scotch straightening mechanism study and system design," *Energy Procedia*, vol. 16, pp. 38–44, 2012.

[7] Z. Q. Zhang, Y. H. Yan, and H. L. Yang, "Modeling of the critical radius for straightening thin-walled tubes with equal curvatures," *Engineering Mechanics*, vol. 32, pp. 207–213, 2015.

[8] Z. Q. Zhang, Y. H. Yan, H. L. Yang et al., "Numerical solution and mechanical modeling of the intermesh for continuous straightening a thin-walled tube in plane stress," *Chinese*

Journal of Computational Mechanics, vol. 32, pp. 212–219, 2015.

[9] Z.-Q. Zhang, "Prediction of maximum section flattening of thin-walled circular steel tube in continuous rotary straightening process," *Journal of Iron and Steel Research International*, vol. 23, no. 8, pp. 745–755, 2016.

[10] Z. Q. Zhang, Y. H. Yan, and H. L. Yang, "A simplified model of maximum cross-section flattening in continuous rotary straightening process of thin-walled circular steel tubes," *Journal of Materials Processing Technology*, vol. 238, pp. 305–314, 2016.

[11] J. Yin, J. Zhao, S.-Y. Wang, X.-S. Wan, and Y.-L. Li, "Principle of multi-roller straightening process and quantitative resolutions of straightening strategies," *Journal of Iron and Steel Research International*, vol. 21, no. 9, pp. 823–829, 2014.

[12] R. Kaiser, T. Hatzenbichler, B. Buchmayr, and T. Antretter, "Simulation of the roller straightening process with respect to residual stresses and the curvature trend," *International Conference on Residual Stresses*, vol. 9, no. 9, pp. 768-769, 2014.

[13] K. Wang, B. Wang, and C. Yang, "Research on the multi-step straightening for the elevator guide rail," *Procedia Engineering*, vol. 16, pp. 459–466, 2011.

[14] L. Madej, K. Muszka, K. Perzyński, J. Majta, and M. Pietrzyk, "Computer aided development of the levelling technology for flat products," *CIRP Annals*, vol. 60, no. 1, pp. 291–294, 2011.

[15] E. Hosseini and M. Kazeminezhad, "Implementation of a constitutive model in finite element method for intense deformation," *Materials & Design*, vol. 32, no. 2, pp. 487–494, 2011.

[16] Z.-F. Liu, Y.-X. Luo, X.-C. Yan, and Y.-Q. Wang, "Boundary determination of leveling capacity for plate roller leveler based on curvature integration method," *Journal of Central South University*, vol. 22, no. 12, pp. 4608–4615, 2015.

[17] Z. Liu, Y. Wang, and X. Yan, "A new model for the plate leveling process based on curvature integration method," *International Journal of Mechanical Sciences*, vol. 54, no. 1, pp. 213–224, 2012.

[18] Y.-Q. Wang, Z.-F. Liu, and X.-C. Yan, "Evaluation of straightening capacity of plate roll straightener," *Journal of Central South University*, vol. 19, no. 9, pp. 2477–2481, 2012.

[19] L. Cui, Q.-Q. Shi, X.-H. Liu, and X.-L. Hu, "Residual curvature of longitudinal profile plate roller in leveling process," *Journal of Iron and Steel Research International*, vol. 20, no. 10, pp. 23–27, 2013.

[20] B.-A. Behrens, T. El Nadi, and R. Krimm, "Development of an analytical 3D-simulation model of the levelling process," *Journal of Materials Processing Technology*, vol. 211, no. 6, pp. 1060–1068, 2011.

[21] W.-H. Chen, J. Liu, Z.-S. Cui, Y.-J. Wang, and Y.-R. Wang, "A 2.5-dimensional analytical model of cold leveling for plates with transverse wave defects," *Journal of Iron and Steel Research International*, vol. 22, no. 8, pp. 664–671, 2015.

[22] R. Brauneis, A. Steinboeck, M. Jochum, and A. Kugi, "A robust real-time model for plate leveling," *IFAC-PapersOnLine*, vol. 51, no. 2, pp. 61–66, 2018.

[23] H. L. Gui, L. F. Ma, X. G. Wang, X. Yang, Q. X. Huang, and Q. Li, "Analysis of the neutral layer offset of bimetal composite plate in the straightening process using boundary element subfield method," *Applied Mathematical Modelling*, vol. 50, pp. 732–740, 2017.

[24] C. Zhang, Y. Zang, B. Guan, and Q. Qin, "Analysis of bimetal composite plate roller leveling process based on curvature integration method," *Journal of Zhejiang University (Engineering Science)*, vol. 51, no. 8, pp. 1575–1586, 2017.

[25] Q.-H. Fan, H. Zhang, X.-C. Jiang, and B.-Z. Tian, "Study on neutral layer offset of high-strength steel plate straightening of excavator's working arm," *Advances in Mechanical Engineering*, vol. 9, no. 7, Article ID 168781401771242, 2017.

[26] M. Baumgart, A. Steinboeck, T. Kiefer, and A. Kugi, "Modelling and experimental validation of the deflection of a leveller for hot heavy plates," *Mathematical and Computer Modelling of Dynamical Systems*, vol. 21, no. 3, pp. 202–227, 2015.

[27] Q. Zhang, T. Liu, and Z. Jianru, "Simulation of wide steel strip deformation during tension levelling by finite element method," *Chinese Journal of Mechanical Engineering*, vol. 44, no. 9, pp. 236–240, 2008.

[28] E. A. Maksimov, R. L. Shatalov, and N. N. Litvinova, "Study of the tractive forces applied to galvanized strip on a straightening machine in a continuous hot-galvanizing unit," *Metallurgist*, vol. 58, no. 5-6, pp. 415–420, 2014.

[29] G. Stadler, A. Steinboeck, and A. Kugi, "Control of curvature and contact force of a metal strip at the strip-roll contact point," *IFAC-PapersOnLine*, vol. 50, no. 1, pp. 11325–11330, 2017.

[30] M. Grüber and G. Hirt, "Numerical investigation of a process control for the roller levelling process based on a force measurement," *Materials Science Forum*, vol. 854, pp. 249–254, 2016.

[31] M. Grüber and G. Hirt, "A strategy for the controlled setting of flatness and residual stress distribution in sheet metals via roller levelling," *Procedia Engineering*, vol. 207, pp. 1332–1337, 2017.

[32] R.-P. Nikula and K. Karioja, "Steel Grade Specific Stress Predictions to Support Roller Leveller Maintenance," in *Proceedings of the First World Congress on Condition Monitoring*, pp. 13–16, London, UK, June 2017.

[33] R.-P. Nikula, K. Karioja, K. Leiviskä, and E. Juuso, "Prediction of mechanical stress in roller leveler based on vibration measurements and steel strip properties," *Journal of Intelligent Manufacturing*, vol. 30, no. 4, pp. 1563–1579, 2017.

[34] J. Lian, *Straightening Theory and Coiling Theory*, China Machine Press, Beijing, China, 2011.

[35] E. Doege, R. Menz, and S. Huinink, "Analysis of the levelling process based upon an analytic forming model," *CIRP Annals*, vol. 51, no. 1, pp. 191–194, 2002.

[36] Z. Y. Hu, G. Yi, and S. Y. Zhang, "Hierarchical evolutionary approach for design structure matrix oriented to complex electromechanical system modeling," *Computer Integrated Manufacturing System*, vol. 19, no. 10, pp. 2385–2393, 2013, in Chinese.